

Showcasing research from the Deutsche Forschungsgemeinschaft (DFG)-funded transregional collaborative research center SFB/TRR 88 "3MET": Franziska Völcker and Peter W. Roesky, Karlsruher Institut Für Technologie (KIT).

Bimetallic rare-earth/platinum complexes ligated by phosphinoamides

The heterometallic early-late 5d/4f binuclear phosphinoamido Ln/Pt(0) complexes $[(\text{Ph}_2\text{PNHPh})\text{Pt}\{\mu-(\text{Ph}_2\text{PNPh})\}_3\text{Ln}(\mu\text{-Cl})\text{-Li}(\text{THF})_3]$ and $[(\text{Ph}_2\text{PNHPh})\text{Pt}\{\mu-(\text{Ph}_2\text{PNPh})\}_3\text{Ln}\{\eta^2-(\text{Ph}_2\text{PNPh})\}]\text{-[Li}(\text{THF})_4]$ (Ln = Y, Lu) were synthesized.

As featured in:



See Franziska Völcker and Peter W. Roesky *Dalton Trans.*, 2016, 45, 9429.



www.rsc.org/dalton

Registered charity number: 207890



Cite this: *Dalton Trans.*, 2016, **45**, 9429

Received 29th January 2016,
Accepted 9th March 2016

DOI: 10.1039/c6dt00417b

www.rsc.org/dalton

Bimetallic rare-earth/platinum complexes ligated by phosphinoamides†

Franziska Völcker and Peter W. Roesky*

The heterometallic early-late 5d/4f binuclear phosphinoamido Ln/Pt(0) complexes $[(\text{Ph}_2\text{PNHPh})\text{Pt}\{\mu-(\text{Ph}_2\text{PNPh})\}_3\text{Ln}(\mu\text{-Cl})\text{Li}(\text{THF})_3]$ (Ln = Y (**1a**), Lu (**1b**)) were obtained by reaction of $[\text{Li}(\text{THF})_4][(\text{Ph}_2\text{PNPh})_4\text{Ln}]$ (Ln = Y, Lu) with the Pt(0) complex $[\text{Pt}(\text{tBu}_3\text{P})_2]$ in the presence of LiCl. In the absence of LiCl the corresponding Ln/Pt(0) complexes $[(\text{Ph}_2\text{PNHPh})\text{Pt}\{\mu-(\text{Ph}_2\text{PNPh})\}_3\text{Ln}(\eta^2-(\text{Ph}_2\text{PNPh}))][\text{Li}(\text{THF})_4]$ (Ln = Y (**2a**), Lu (**2b**)) were isolated. Both kind of complexes decompose in solution. The Pt(0) complex $[\text{Pt}(\text{Ph}_2\text{PNHPh})_4]$ (**3**) was identified as one of these decomposition products.

Introduction

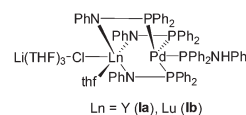
Homo- and heterobimetallic complexes have been studied for catalytic application and small molecule activation over recent years.^{1,2} Some of these compounds show cooperative and synergistic effects that can arise from the simultaneous or consecutive action of different metal centers in different media.² Inspired by nature, the concept of cooperative bimetallic catalysis has been employed for the synthesis of numerous artificial catalysts. The emerging field of homo- and heterobimetallic and polymetallic catalyst systems has been summarized in several review articles recently.^{2–6} Within this area heterobimetallic early/late complexes^{7,8} having interactions between a hard Lewis acidic early metal atom and a soft Lewis basic late metal atom are of interest because they feature significantly different reaction sites. This makes them interesting for potential applications in catalysis.⁹ For the synthesis of heterobimetallic early/late complexes carbonyl-, hydride-, halide-, selenide-, and thiolate ligands were used as bridging ligands.¹ Recently, Thomas *et al.* reported heterobimetallic transition metal complexes with metal-to-metal bonds bridged by phosphinoamido ligands.⁹ The known combinations of metals realized by this concept are bimetallic complexes, *e.g.* Co/Ti,^{10,11} Co/Zr,^{9,12–16} Co/Hf,¹⁷ Pt/Zr,¹⁸ V/Fe,¹⁹ Nb/Co,²⁰ Ta/Co,²⁰ and Co/U.²¹

In contrast to transition metal complexes, heterobimetallic early/late complexes^{7,8} containing rare-earth metals are far less common. Thus, only few complexes of the rare-earth elements with non-supported metal-to-metal bonds to a transition metal

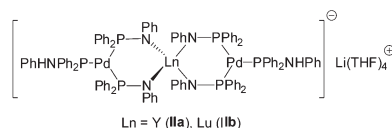
were reported.¹⁷ Examples include complexes with Lu–Ru,²² Ln–Re (Ln = La, Sm, Yb, Lu),^{20,23–25} Nd–Fe,²⁶ and Yb–Fe bonds.²⁷

Heterobimetallic compounds, which have a rare-earth metal atom and a rhodium, palladium, or platinum atom in close proximity (distance of less than 3.5 Å) are also not very common. Kempe *et al.* reported some Nd/Rh and Nd/Pd complexes,^{28,29} in which the metals are brought closely together by bis(aminopyridinato) ligands. Hou *et al.* recently reported heterobimetallic rare-earth metal/platinum complexes. In these half-sandwich rare-earth metal alkyl complexes Cp ligands with a phosphine side arm were used.³⁰

As seen by these few examples one of the big challenges that still remain is the synthesis of heterobimetallic early/late complexes containing rare-earth metals. Lately, we reported the synthesis of the heterometallic early-late 4d/4f bi- and trinuclear phosphinoamido Ln/Pd(0) complexes $[(\text{Ph}_2\text{PNHPh})\text{Pd}\{\mu-(\text{Ph}_2\text{PNPh})\}_3\text{Ln}(\mu\text{-Cl})\text{Li}(\text{THF})_3]$ (Ln = Y (**1a**), Lu (**1b**)) and $[\text{Li}(\text{THF})_4][\{(\text{Ph}_2\text{PNHPh})\text{Pd}\}_2\{\mu-(\text{Ph}_2\text{PNPh})\}_4\text{Ln}]$ (Ln = Y (**IIa**), Lu (**IIb**)) (Scheme 1).^{31,32} The latter compounds are the first early/late trimetallic phosphinoamido complexes. Compounds **1a,b** and **IIa,b** were obtained by reaction of $[\text{Li}(\text{THF})_4]$



Ln = Y (**1a**), Lu (**1b**)



Ln = Y (**IIa**), Lu (**IIb**)

Scheme 1 Bi- and trinuclear phosphinoamido Ln/Pd(0) complexes.³¹

Institut für Anorganische Chemie, Karlsruher Institut für Technologie (KIT), Engesserstr. 15, Geb. 30.45, 76131 Karlsruhe, Germany. E-mail: roesky@kit.edu
† Electronic supplementary information (ESI) available: Details of experimental and crystallographic studies. CCDC 1450174–1450176. For ESI and crystallographic data in CIF or other electronic format see DOI: 10.1039/c6dt00417b

$[(\text{Ph}_2\text{PNPh})_4\text{Ln}]$ ($\text{Ln} = \text{Y}, \text{Lu}$)^{33–36} with the palladium allyl complex $[\text{Pd}_2(\text{C}_3\text{H}_5)_2\text{Cl}_2]$. A reduction of the palladium atoms was observed upon the formation of the bi- and trimetallic compounds **1a,b** and **1a,b**. Although the metal atoms are forced into close proximity by the phosphinoamido ligands, quantum chemical calculations of $[(\text{Ph}_2\text{PNHPh})\text{Pd}\{\mu-(\text{Ph}_2\text{PNPh})\}_3\text{Lu}(\mu\text{-Cl})\text{Li}(\text{THF})_3]$ showed only weak metal-to-metal interactions.^{31,32}

Motivated by these initial results, we were interested in extending our studies on heterobimetallic early/late complexes containing rare-earth metals. Herein, we now report heterobimetallic rare-earth metal/platinum complexes bridged by phosphinoamido ligands.

Results and discussion

The palladium complexes **1a,b** were obtained most efficiently by the addition of LiCl to the reaction mixture giving the desired complexes. In a similar protocol, the reaction of $[\text{Li}(\text{THF})_4][(\text{Ph}_2\text{PNPh})_4\text{Ln}]$ ($\text{Ln} = \text{Y}, \text{Lu}$) with the Pt(0) precursor $[\text{Pt}(\text{P}(\text{tBu})_3)_2]$ in the presence of LiCl resulted after crystallization in the Ln/Pt(0) complexes $[(\text{Ph}_2\text{PNHPh})\text{Pt}\{\mu-(\text{Ph}_2\text{PNPh})\}_3\text{Ln}(\mu\text{-Cl})\text{Li}(\text{THF})_3]$ ($\text{Ln} = \text{Y}$ (**1a**), Lu (**1b**)) in moderate yields (Scheme 2). Formally, the Pt atom inserts into the weak Ln–P bonds forming the desired heterobimetallic complexes. We presume that some decomposition occurs and $\text{Ph}_2\text{PN}(\text{H})\text{Ph}$, which is coordinated to the Pt atom, is formed as a side-product. In contrast to the formation of the Pd(0) complexes **1a,b**, which were obtained only in a reductive approach from a Pd(II) source, compounds **1a,b** are directly accessible from a Pt(0) precursor. By using Pt(II) salts as starting material no traceable products were obtained.

Although the reactions leading to **1a** and **1b** seem, at first glance, quiet similar, their accessibility is significantly different. Whereas **1a** was obtained straight forward in a reproducible way, the preparation of **1b** is more difficult.

Single crystals of **1a,b** suitable for X-ray diffraction were obtained by crystallization from THF/toluene/pentane (Fig. 1 and S1†). Compounds **1a,b** crystallize in the triclinic space group $P\bar{1}$ with one molecule of the complexes in the asymmetric unit. Furthermore, one molecule of THF and toluene were localized each in the asymmetric unit. The toluene molecule in **1a** showed a strong disorder and was thus suppressed by using Olex solvent mask.³⁷ In both compounds, the Ln and the Pt atoms are forced in close proximity by three bridging $\mu-(\text{Ph}_2\text{PNPh})$ ligands. As expected the soft P atom binds to the Pt atom, whereas the hard nitrogen atoms coordinate to the rare-earth metal atom. In both compounds, the Li atom is

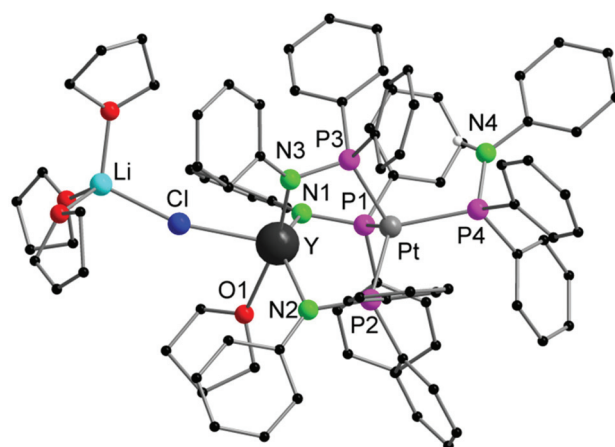
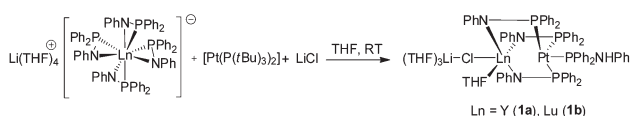


Fig. 1 Solid-state structure of **1a**. Carbon bound hydrogen atoms are omitted for clarity. Compound **1b** is isostructural. Selected bond lengths [Å], angles [°]: **1a**: Pt–Y 3.0063(8), Pt–P1 2.3206(13), Pt–P2 2.3363(12), Pt–P3 2.3368(11), Pt–P4 2.3477(12), Y–Cl 2.6525(14), Y–O1 2.471(3), Y–N1 2.347(3), Y–N2 2.291(3), Y–N3 2.325(3), Cl–Li 2.353(2), P1–N1 1.678(3), P2–N2 1.665(3), P3–N3 1.676(3), P4–N4 1.677(4); P1–Pt–P2 116.56(4), P1–Pt–P3 106.95(5), P1–Pt–P4 104.66(4), P2–Pt–P3 106.03(4), P2–Pt–P4 113.45(5), P3–Pt–P4 108.87(4), N1–Y–N2 130.76(12), N1–Y–N3 108.52(11), N2–Y–N3 97.97(12), N1–Y–Cl 106.17(9), N2–Y–Cl 116.47(9), N3–Y–Cl 86.40(9), O1–Y–Cl 81.61(8), N1–Y–O1 81.56(11), N2–Y–O1 81.44(11), N3–Y–O1 166.19(11). **1b** (see Fig. S1†) Pt–Lu 2.9523(9), Pt–P1 2.321(2), Pt–P2 2.337(2), Pt–P3 2.307(2), Pt–P4 2.324(2), Lu–Cl 2.601(2), Lu–O1 2.442(6), Lu–N1 2.269(6), Lu–N2 2.242(6), Lu–N3 2.297(6), Lu–P1 3.085(2), Lu–P2 3.107(2), Lu–P3 3.109(2), Cl–Li 2.31(2), P1–N1 1.658(7), P2–N2 1.650(6), P3–N3 1.664(6), P4–N4 1.683(7); P1–Pt–P2 106.10(8), P1–Pt–P3 106.85(8), P1–Pt–P4 107.98(9), P2–Pt–P3 116.32(8), P3–Pt–P4 104.49(8), N1–Lu–N2 97.7(2), N1–Lu–N3 110.1(2), N2–Lu–N3 131.5(2), N1–Lu–Cl 85.5(2), N2–Lu–Cl 116.2(2), N3–Lu–Cl 105.2(2), N1–Lu–Cl 85.5(2), N2–Lu–Cl 116.2(2), N3–Lu–O1 81.4(2).

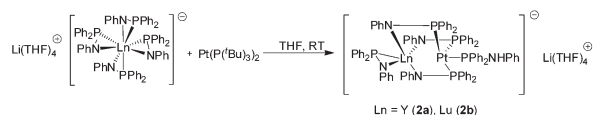
coordinated to the Ln atom *via* a $\mu\text{-Cl}$ bridge. The rare-earth atoms are thus five-fold coordinated by three Ph_2PNPh ligands, one molecule of THF and the chlorine atom. A distorted trigonal bipyramidal coordination polyhedron with the THF oxygen atom and N3 in the axis is formed. The Ln–N bond distances (**1a**: 2.291(3) Å–2.347(3); **1b**: 2.242(6)–2.297(6) Å) are in the range of **1a,b** (av. 2.317 Å (**1a**), 2.262 Å (**1b**)).³¹ The Ln–Cl bond lengths are 2.6525(14) Å (**1a**), 2.601(2) Å (**1b**). The Pt atom is four-fold coordinated by the phosphorous atoms of three $\mu-(\text{Ph}_2\text{PNPh})$ ligands and one Ph_2PNHPh ligand. A distorted tetrahedral coordination polyhedron is formed by the four P atoms around the Pt atom. The Pt–P bond distances are av. 2.3354 Å (**1a**), 2.328 Å (**1b**). Although the Pt atom has a slightly larger van-der-Waals radius in comparison to Pd, the Ln–Pt distances in **1a,b** (3.0063(8) Å (**1a**), 2.9523(9) Å (**1b**)) are in the range of those in the Ln–Pd complexes **1a,b** (2.9898(6) Å (**1a**), 2.9031(11) Å (**1b**)). This is clearly showing that the three $\mu-(\text{Ph}_2\text{PNPh})$ ligands are forcing the metal atoms into close proximity.

Since traces of LiCl within the starting material $[\text{Li}(\text{THF})_4][(\text{Ph}_2\text{PNPh})_4\text{Y}]$ ($\text{Ln} = \text{Y}, \text{Lu}$) resulted in the reaction with $[\text{Pt}(\text{P}(\text{tBu})_3)_2]$ in **1a**, we improved our synthesis of $[\text{Li}(\text{THF})_4]$



Scheme 2 Synthesis of **1a,b**.





Scheme 3 Synthesis of 2a,b.

$[(\text{Ph}_2\text{PNPh})_4\text{Ln}]$. $[\text{Li}(\text{THF})_4][(\text{Ph}_2\text{PNPh})_4\text{Ln}]^{33-36}$ is obtained by the reaction of LnCl_3 with LiPPh_2NPh in a 1 : 4 molar ratio. Usually, the product can be directly obtained by crystallization from THF/*n*-pentane. But obviously the bulk material is sometimes contaminated with traces of LiCl . By extraction of the crude product with toluene before crystallization, the contamination of the product with LiCl is avoided. The desired product is thus obtained in higher purity.

Reaction of very pure $[\text{Li}(\text{THF})_4][(\text{Ph}_2\text{PNPh})_4\text{Ln}]$ ($\text{Ln} = \text{Y}, \text{Lu}$) with $[\text{Pt}(\text{P}(\text{tBu})_3)_2]$ gave the bimetallic compounds $[(\text{Ph}_2\text{PNHPh})\text{Pt}\{\mu-(\text{Ph}_2\text{PNPh})\}_3\text{Ln}\{\eta^2-(\text{Ph}_2\text{PNPh})\}][\text{Li}(\text{THF})_4]$ ($\text{Ln} = \text{Y}$ (**2a**), Lu (**2b**)) as yellow crystals (Scheme 3). The formation of **2a,b** is similar to **1a,b**. Again, the $\text{Pt}(0)$ atom formally inserts into three of the $\text{Ln}-\text{P}$ bonds. The fourth PPh_2NPh ligand remains in a η^2 -coordination mode on the Ln atom. The Pt atom forms a similar coordination polyhedron as observed in **1a,b**.

As seen for the formation of compounds **1a,b**, there is a difference in reactivity. Upon workup, **2a** was obtained as pure material in single crystalline form and complete characterization was possible. In contrast, the reaction leading to **2b** is not quantitative. Even after prolonged reaction times the workup of **2b** resulted in a mixture of the desired product and $[\text{Li}(\text{THF})_4][(\text{Ph}_2\text{PNPh})_4\text{Lu}]$. The solid-state structures of both **2a** and **2b** were established by single crystal X-ray diffraction but for **2b** no further analytical data could be collected.

Compound **2a** crystallizes in the monoclinic space group *Cc* with one molecule of the complexes in the asymmetric unit. Although the X-ray data collected from **2b** was very poor, its composition was deduced from the difference Fourier map (Fig. S2†). Bond angles and distances of **2b** thus are not discussed. Compounds **2a,b** consist of a $[(\text{Ph}_2\text{PNHPh})\text{Pt}\{\mu-(\text{Ph}_2\text{PNPh})\}_3\text{Ln}\{\eta^2-(\text{Ph}_2\text{PNPh})\}]^-$ anion and a $[\text{Li}(\text{THF})_4]^+$ cation (Fig. 2). As seen in **1a,b** the Pt atom in **2a,b** is four fold-coordinated by three $\mu-(\text{Ph}_2\text{PNPh})$ and one Ph_2PNHPh ligand resulting in a distorted tetrahedral coordination polyhedron, which is formed by the four P atoms around the Pt atom. Since the central part of the $[(\text{Ph}_2\text{PNHPh})\text{Pt}\{\mu-(\text{Ph}_2\text{PNPh})\}_3\text{Ln}\{\eta^2-(\text{Ph}_2\text{PNPh})\}]^-$ anion is similar to **1a,b** the $\text{Y}-\text{Pt}$ distance in **2a** (3.032(2) Å) is as expected. The main difference between **2a,b** and **1a,b** is the coordination sphere of the Ln atom. Instead of a molecule of THF and a chlorine atom, which are bound to the Ln atom in **1a,b**, a η^2 -coordinated PPh_2NPh ligand is bound to the lanthanide atom in **2a,b**. Additionally, the N atoms of three bridging $\mu-(\text{Ph}_2\text{PNPh})$ ligands coordinate to the Ln atom resulting in a five-fold coordinated metal atom. The $\text{Ln}-\text{N}$ bonds in **2a** range from 2.285(12) Å to 2.301(2) Å.

As observed for **1a,b**, also the Pt complexes **1a,b** and **2a,b** decompose in solution. This is one explanation for the low yields and the formation of the protonated ligand PPh_2NHPh .

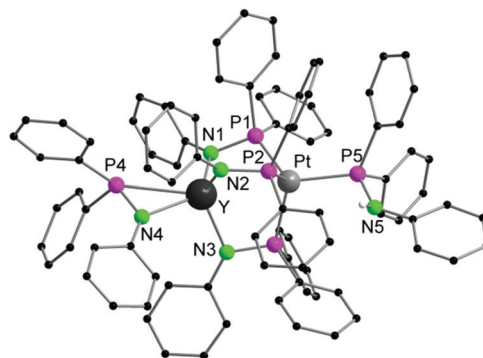


Fig. 2 Solid-state structure of the anion of **2a**. Carbon bound hydrogen atoms are omitted for clarity. Compound **2b** is similar. Selected bond lengths [Å], angles [°]: **2a**: $\text{Pt}-\text{Y}$ 3.032(2), $\text{Pt}-\text{P1}$ 2.367(4), $\text{Pt}-\text{P2}$ 2.301(4), $\text{Pt}-\text{P3}$ 2.330(4), $\text{Pt}-\text{P5}$ 2.371(4), $\text{Y}-\text{P4}$ 2.931(4), $\text{Y}-\text{N1}$ 2.285(12), $\text{Y}-\text{N2}$ 2.309(13), $\text{Y}-\text{N3}$ 2.300(15), $\text{Y}-\text{N4}$ 2.315(15), $\text{P1}-\text{N1}$ 1.659(13), $\text{P2}-\text{N2}$ 1.649(13), $\text{P3}-\text{N3}$ 1.663(14), $\text{P4}-\text{N4}$ 1.643(12); $\text{P1}-\text{Pt}-\text{P5}$ 114.73(2), $\text{P2}-\text{Pt}-\text{P1}$ 107.47(14), $\text{P2}-\text{Pt}-\text{P3}$ 111.18(15), $\text{P2}-\text{Pt}-\text{P5}$ 105.54(15), $\text{P3}-\text{Pt}-\text{P1}$ 109.77(14), $\text{P3}-\text{Pt}-\text{P5}$ 108.12(15), $\text{N4}-\text{Y}-\text{P4}$ 34.0(3), $\text{N1}-\text{Y}-\text{N2}$ 114.9(5), $\text{N1}-\text{Y}-\text{N3}$ 103.0(5), $\text{N1}-\text{Y}-\text{N4}$ 126.2(4), $\text{N3}-\text{Y}-\text{N2}$ 120.0(5), $\text{N3}-\text{Y}-\text{N4}$ 99.1(5).

The $^{31}\text{P}\{^1\text{H}\}$ NMR spectra show fast decomposition of all compounds in various solvents. In d_8 -THF a large number of signals were observed. In C_6D_6 major signals with the corresponding ^{195}Pt satellites were observed in the $^{31}\text{P}\{^1\text{H}\}$ NMR spectra of **1a,b** and **2a** (Fig. S3–S5†). However, the ratio varies from sample to sample and further decomposition signals were sometimes also observed as well. As a result of the fast decomposition, there remain significant uncertainties of the correct assignment of the signals. A ^1H , ^{195}Pt HMBC NMR spectrum was also not conclusive.

One of the decomposition products could be identified. From a saturated solution of **1a** in d_8 -THF the $\text{Pt}(0)$ complex $[\text{Pt}(\text{PPh}_2\text{NHPh})_4]$ (**3**) crystallized once in a NMR tube. Although **3** was not fully characterized and the X-ray data collected was poor, its composition was deduced from the difference Fourier map (Fig. 3) giving thus some insight into the decomposition pathway. Moreover, **3** was also identified by ESI-MS

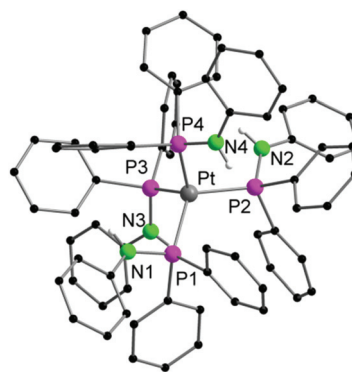


Fig. 3 Solid-state structure of the anion of **3**. Carbon bound hydrogen atoms are omitted for clarity.



spectroscopy of a solution of **1a**. In **3**, the Pt(0) atom is four-fold coordinated by the phosphorous atoms of four PPh₂NHPh ligands in a tetrahedral fashion. The only slightly related phosphinoamido structure of platinum reported in the literature is found in the Pt(i) species [Pt(NPhPPh₂)(HNPhPPh₂)]₂, having a Pt–Pt bond.³⁸

Experimental³²

All manipulations of air-sensitive materials were performed with the rigorous exclusion of oxygen and moisture in Schlenk-type glassware either on a dual manifold Schlenk line, interfaced to a high vacuum (10^{−3} torr) line, or in an argon-filled MBraun glove box. Elemental analyses were carried out with an Elementar vario Micro Cube. Hydrocarbon solvents were predried using an MBraun solvent purification system (SPS-800) and then they were degassed, dried and stored *in vacuo* over LiAlH₄. Tetrahydrofuran was distilled under nitrogen from potassium before storage over LiAlH₄. Deuterated solvents were obtained from Euro-Isotop (99.5 atom% D) and were degassed, dried and stored *in vacuo* over Na/K alloy in resealable flasks. ¹H and ³¹P{¹H} NMR spectra were recorded on a Bruker Avance II 300 MHz or Avance 400 MHz. ¹H chemical shifts were referenced to the residual deuterated solvents and are reported relative to tetramethylsilane, ³¹P{¹H} was referenced to external 85% phosphoric acid. IR spectra were obtained on a Bruker Tensor 37 FTIR spectrometer equipped with a room temperature DLATGS detector and a diamond ATR (attenuated total reflection) unit. Raman spectra were recorded on a Bruker MultiRAM spectrometer.

¹⁹⁵Pt-NMR spectra were recorded at 300 K on a Bruker Avance II 600 spectrometer using a double-resonance ¹H-BBI probe head. Platinum frequencies were determined by an ultrabroadband version of a gradient selected ¹H, ¹⁹⁵Pt-HMBC.³⁹ Due to the very large chemical shift range of platinum complexes (15 000 ppm, 1.94 MHz @ 14.1 T), it is not possible to cover this range in one conventional experiment. Conventional experiments are acquired with hard pulses that can excite bandwidth of about 50 kHz. Broadband spectra are achieved *via* application of broadband saturation pulses on platinum, which have been designed by optimal control derived optimizations.^{40–45}

[Pt(P(*t*Bu)₃)₂] (ABCR) was used as purchased from commercial sources without further purification. [Li(THF)₄][(Ph₂PNPh)₄Ln] (Ln = Y, Lu),^{31,34} LnCl₃ (Ln = Y, Lu),⁴⁶ and LiPh₂NPh^{38,47} were prepared according to literature procedure.

[(Ph₂PNHPh)Pt{μ-(Ph₂PNPh)}₃Y(μ-Cl)Li(thf)₃] (**1a**)

15 ml THF was condensed at −78 °C onto a mixture of 186 mg (0.125 mmol) [Li(THF)₄][(Ph₂PNPh)₄Y], 75 mg (0.125 mmol) bis(*tri-tert*-butylphosphine)platinum(0) and 5.3 mg (0.125 mmol) anhydrous lithium chloride. The orange solution was stirred for 3 h at ambient temperature. After the reaction period the solution was concentrated and 10 ml toluene was

condensed onto the mixture. After filtration, the THF/toluene mixture was layered with toluene and with *n*-pentane. After one day 50 mg (0.035 mmol, 28%) of yellow crystals were formed. In a few cases the formation of colorless crystals of [Li(THF)₄][(Ph₂PNPh)₄Y] was observed, which could be separated from the yellow crystals in the glove box.

IR (ATR): $\tilde{\nu}$ (cm^{−1}) = 3380 (w), 3044 (w), 2866 (w), 1598 (m), 1494 (m), 1472 (m), 1431 (m), 1389 (m), 1280 (m), 1225 (m), 1181 (w), 1155 (w), 1092 (m), 1066 (m), 1028 (m), 996 (m), 894 (m), 741 (s), 691 (s), 617 (m), 593 (s), 508 (s), 463 (s), 429 (s). – Raman: $\tilde{\nu}$ (cm^{−1}) = 3060 (m), 3023 (w), 2886 (w), 1585 (vs), 1570 (m), 1479 (w), 1445 (w), 1433 (w), 1393 (w), 1324 (w), 1282 (w), 1246 (w), 1183 (w), 1155 (w), 1088 (s), 1030 (s), 1001 (vs), 927 (w), 849 (w), 794 (w), 769 (w), 741 (w), 695 (w), 641 (w), 619 (w), 597 (w), 530 (m), 509 (w), 486 (w), 463 (w), 442 (w), 430 (w), 408 (w), 272 (w), 227 (w), 187 (m), 170 (m). – C₈₈H₉₃ClLiN₄O₄P₄PtY (1720.98): calc. C 61.41, H 5.45, N 3.26; exp. C 61.38, H 5.45, N 2.95.

[(Ph₂PNHPh)Pt{μ-(Ph₂PNPh)}₃Lu(μ-Cl)Li(thf)₃] (**1b**)

15 ml THF was condensed at −78 °C onto a mixture of 200 mg (0.127 mmol) [Li(THF)₄][(Ph₂PNPh)₄Lu], 76 mg (0.127 mmol) bis(*tri-tert*-butylphosphine)platinum(0) and 2.7 mg (0.063 mmol) anhydrous lithium chloride. The orange solution was stirred over night at ambient temperature. After the reaction period the solution was concentrated and 10 ml toluene was condensed onto the mixture. After filtration, the THF/toluene mixture was layered with toluene and with *n*-pentane. After one day 36 mg (0.020 mmol, 16%) of yellow crystals were formed. Additionally the formation of colorless crystals of [Li(THF)₄][(PPh₂NPh)₄Lu] was observed, which could be separated from the yellow crystals in the glove box. When the product was recrystallized several times, crystals of **2b** were also formed.

IR (ATR): $\tilde{\nu}$ (cm^{−1}) = 3381 (w), 3047 (w), 2972 (w), 2865 (w), 1598 (m), 1494 (m), 1473 (m), 1432 (m), 1390 (m), 1280 (s), 1226 (m), 1181 (m), 1155 (w), 1092 (m), 1066 (m), 1028 (m), 996 (m), 894 (s), 741 (s), 691 (vs), 630 (m), 617 (m), 593 (s), 507 (vs), 475 (s), 464 (vs), 430 (s). – Raman: $\tilde{\nu}$ (cm^{−1}) = 3057 (m), 2980 (w), 2881 (w), 1585 (vs), 1570 (m), 1481 (w), 1445 (w), 1277 (w), 1239 (w), 1181 (w), 1156 (w), 1091 (s), 1030 (s), 1001 (vs), 918 (w), 793 (w), 741 (w), 695 (w), 642 (w), 619 (w), 597 (w), 530 (m), 480 (w), 439 (w), 407 (w), 269 (w), 227 (w), 170 (m). – EA: C₈₈H₉₃ClLiN₄O₄P₄PtLu (1807.04): calc. C 58.49, H 5.19, N 3.10; exp. C 58.37, H 5.09, N 2.95.

Improved synthesis of [Li(thf)₄][Ln(Ph₂PNPh)₄] (Ln = Y, Lu) to avoid traces of LiCl³⁴

Ln = Y. 15 ml THF was condensed at −78 °C onto a mixture of 120 mg (0.615 mmol) YCl₃ and 696 mg (2.46 mmol) LiPh₂NPh. The solution was stirred over night at ambient temperature. After removing the solvent the residue was dissolved in 20 ml toluene and the solution was filtered. The solvent was removed and the oily residue was washed with *n*-pentane. The obtained solid was dissolved in THF and *n*-pentane was layered on top of the solution. After one day



200 mg (0.134 mmol, 22%) colorless crystals could be obtained.

Ln = Lu. 200 mg (0.711 mmol) LuCl_3 and 805 mg (2.84 mmol) LiPh_2PNPh . Yield: 297 mg (0.212 mmol, 30%).

$[(\text{Ph}_2\text{PNHPh})\text{Pt}\{\mu\text{-(Ph}_2\text{PNPh)}\}_3\text{Y}\{\eta^2\text{-(Ph}_2\text{PNPh)}\}][\text{Li}(\text{thf})_4]$ (2a**)**

15 ml of THF was condensed at -78°C onto a mixture of 186 mg (0.125 mmol) $[\text{Li}(\text{thf})_4][(\text{Ph}_2\text{PNPh})_4\text{Y}]$ and 75 mg (0.125 mmol) bis(tri-*tert*-butylphosphine)-platinum(0). The mixture was stirred for 4 h at ambient temperature. After the reaction period the solution was concentrated and 10 ml of toluene was condensed onto the mixture. After filtration, the THF/toluene mixture was layered with toluene and with *n*-pentane. After one day 23 mg (0.012 mmol, 9%) yellow crystals were formed.

IR (ATR): $\tilde{\nu}$ (cm^{-1}) = 3381 (w), 3045 (w), 2924 (w), 2854 (w), 1598 (m), 1494 (m), 1472 (m), 1432 (m), 1389 (m), 1280 (m), 1226 (m), 1180 (w), 1155 (w), 1092 (m), 1066 (m), 1027 (m), 996 (m), 894 (m), 822 (w), 740 (s), 691 (s) 617 (m), 593 (s), 507 (s), 464 (s), 429 (s). – Raman: $\tilde{\nu}$ (cm^{-1}) = 3056 (s), 1585 (vs), 1476 (w), 1433 (w), 1396 (w), 1284 (w), 1234 (w), 1186 (w), 1158 (w), 1093 (m), 1031 (m), 1000 (vs), 898 (w), 800 (w), 769 (w), 698 (w), 619 (w), 525 (w), 487 (w), 412 (w), 255 (w), 225 (w), 194 (w), 173 (w). – EA: $\text{C}_{106}\text{H}_{109}\text{LiN}_5\text{O}_4\text{P}_5\text{PtY}$ (1962.83): calc: C 64.86, H 5.60, N 3.57; exp: C 64.11, H 5.77, N 3.21.

$[(\text{Ph}_2\text{PNHPh})\text{Pt}\{\mu\text{-(Ph}_2\text{PNPh)}\}_3\text{Lu}\{\eta^2\text{-(Ph}_2\text{PNPh)}\}][\text{Li}(\text{thf})_4]$ (2b**)**

15 ml of THF was condensed at -78°C onto a mixture of 140 mg (0.089 mmol) $[\text{Li}(\text{thf})_4][(\text{Ph}_2\text{PNPh})_4\text{Lu}]$ and 53 mg (0.089 mmol) bis(tri-*tert*-butylphosphine)platinum(0). The mixture was stirred for 2 days at ambient temperature. After the reaction period the solution was concentrated and 10 ml of toluene was condensed onto the mixture. After filtration the THF/toluene mixture was layered with toluene and with *n*-pentane. After two times of recrystallization yellow (**2b**) and colourless crystals of $[\text{Li}(\text{THF})_4][(\text{PPh}_2\text{NPh})_4\text{Lu}]$ could be obtained, which could not be separated from each other.

X-Ray-crystallographic studies of 1a, 1b, 2a, 2b and 3

A suitable crystal was covered in mineral oil (Aldrich) and mounted on a glass fiber. The crystal was transferred directly to the cold stream of a STOE IPDS 2 or STOE StadiVari diffractometer.

All structures were solved using SHELXS-2013.⁴⁸ The remaining non-hydrogen atoms were located from difference Fourier map calculations. The refinements were carried out by using full-matrix least-squares techniques on F , minimizing the function $(F_o - F_c)^2$, where the weight is defined as $4F_o^2/2(F_o^2)$ and F_o and F_c are the observed and calculated structure factor amplitudes using the program SHELXL-2013.⁴⁸ Carbon-bound hydrogen atom positions were calculated. The locations of the largest peaks in the final difference Fourier map calculation as well as the magnitude of the residual electron densities in each case were of no chemical significance. Positional

parameters, hydrogen atom parameters, thermal parameters, bond lengths and angles have been deposited as ESI.†

Crystallographic data (excluding structure factors) for the structures reported in this paper have been deposited with the Cambridge Crystallographic Data Centre as a supplementary-publication no. CCDC 1450174–1450176.

Crystal data for **1a**: $\text{C}_{88}\text{H}_{93}\text{ClLiN}_4\text{O}_4\text{P}_4\text{PtY}\cdot\text{C}_4\text{H}_8\text{O}$, $M = 1793.03$, $a = 13.302(3) \text{ \AA}$, $b = 15.181(3) \text{ \AA}$, $c = 22.663(5) \text{ \AA}$, $\alpha = 99.59(3)^\circ$, $\beta = 98.88(3)^\circ$, $\gamma = 99.85(3)^\circ$, $V = 4366.3(16) \text{ \AA}^3$, $T = 150(2) \text{ K}$, space group $P\bar{1}$, $Z = 2$, $\mu(\text{Mo K}\alpha) = 2.418 \text{ mm}^{-1}$, 31 469 reflections measured, 15 963 independent reflections ($R_{\text{int}} = 0.0478$). The final R_1 values were 0.0368 ($I > 2\sigma(I)$). The final $wR(F^2)$ values were 0.0918 ($I > 2\sigma(I)$). The final R_1 values were 0.0451 (all data). The final $wR(F^2)$ values were 0.0947 (all data). The goodness of fit on F^2 was 0.988.

Crystal data for **1b**: $\text{C}_{88}\text{H}_{93}\text{ClLiLuN}_4\text{O}_4\text{P}_4\text{Pt}\cdot\text{C}_4\text{H}_8\text{O}\cdot\text{C}_7\text{H}_8$, $M = 1971.23$, $a = 13.388(3) \text{ \AA}$, $b = 15.201(3) \text{ \AA}$, $c = 22.573(5) \text{ \AA}$, $\alpha = 99.85(3)^\circ$, $\beta = 98.77(3)^\circ$, $\gamma = 97.53(3)^\circ$, $V = 4414.6(16) \text{ \AA}^3$, $T = 210(2) \text{ K}$, space group $P\bar{1}$, $Z = 2$, $\mu(\text{Mo K}\alpha) = 2.853 \text{ mm}^{-1}$, 34 017 reflections measured, 17 155 independent reflections ($R_{\text{int}} = 0.0947$). The final R_1 values were 0.0469 ($I > 2\sigma(I)$). The final $wR(F^2)$ values were 0.0629 ($I > 2\sigma(I)$). The final R_1 values were 0.1300 (all data). The final $wR(F^2)$ values were 0.0763 (all data). The goodness of fit on F^2 was 0.649.

Crystal data for **2a**: $\text{C}_{90}\text{H}_{76}\text{N}_5\text{P}_5\text{PtY}\cdot\text{C}_{16}\text{H}_{32}\text{LiO}_4$, $M = 1961.76$, $a = 23.628(5) \text{ \AA}$, $b = 14.886(3) \text{ \AA}$, $c = 28.196(6) \text{ \AA}$, $\beta = 107.47(3)^\circ$, $V = 9459(4) \text{ \AA}^3$, $T = 209 \text{ K}$, space group Cc , $Z = 4$, $\mu(\text{Mo K}\alpha) = 2.22 \text{ mm}^{-1}$, 36 018 reflections measured, 18 329 independent reflections ($R_{\text{int}} = 0.1126$). The final R_1 values were 0.0639 ($I > 2\sigma(I)$). The final $wR(F^2)$ values were 0.1085 ($I > 2\sigma(I)$). The final R_1 values were 0.1064 (all data). The final $wR(F^2)$ values were 0.1212 (all data). The goodness of fit on F^2 was 0.864.

Crystal data for **3**: $\text{C}_{72}\text{H}_{64}\text{N}_4\text{P}_4\text{Pt}\cdot 6(\text{C}_4\text{H}_8\text{O})$, $M = 1736.86$, $a = 18.281(2) \text{ \AA}$, $b = 18.250(2) \text{ \AA}$, $c = 18.261(2) \text{ \AA}$, $\alpha = 104.797(7)^\circ$, $\beta = 104.736(9)^\circ$, $\gamma = 119.060(9)^\circ$, $V = 4603.9(9) \text{ \AA}^3$, $T = 100 \text{ K}$, space group $P\bar{1}$, $Z = 2$. Due to the fast decomposition no full data set could be acquired.

Conclusions

As already noted in our communication on Ln/Pd complexes³¹ the chemistry of heterobimetallic Ln/Pt complexes supported by phosphinoamido ligands is significantly different from the well-established family of heterobimetallic transition metal complexes with phosphinoamido ligands. The most obvious differences are:

1. The Ln/Pd and Ln/Pt phosphinoamido complexes, which were synthesized so far, are significantly less stable than phosphinoamido transition metal complexes, *e.g.* Co/Zr. This hampers an investigation of their reactivity.

2. As shown by our recently reported quantum chemical calculations for **1b**,³¹ the short metal-to-metal distances are a result of ligand effects, rather than of metal–metal bonds.



The lack of significant metal-to-metal interaction is a result of the strong ionic bonding contribution generally observed in rare-earth chemistry. The lack of stability of the heterobimetallic rare-earth/platinum metal complexes supported by phosphinoamido compounds may also be a result of the difference in bonding compared to pure heterobimetallic transition metals.

Acknowledgements

This work was supported by the DFG-funded transregional collaborative research center SFB/TRR 88 "3MET" Project B3. Dr Benjamin Görling is acknowledged for performing Pt-NMR measurements.

Notes and references

- 1 D. W. Stephan, *Coord. Chem. Rev.*, 1989, **95**, 41–107.
- 2 P. Buchwalter, J. Rosé and P. Braunstein, *Chem. Rev.*, 2015, **115**, 28–126.
- 3 M. Weiss and R. Peters, in *Cooperative Catalysis*, ed. R. Peters, Wiley-VCH Verlag GmbH & Co. KGaA, 2015, pp. 227–262, DOI: 10.1002/9783527681020.ch8.
- 4 I. Bratko and M. Gomez, *Dalton Trans.*, 2013, **42**, 10664–10681.
- 5 J. Park and S. Hong, *Chem. Soc. Rev.*, 2012, **41**, 6931–6943.
- 6 J. I. van der Vlugt, *Eur. J. Inorg. Chem.*, 2012, **2012**, 363–375.
- 7 L. H. Gade, *Angew. Chem., Int. Ed.*, 2000, **39**, 2658–2678.
- 8 N. Wheatley and P. Kalck, *Chem. Rev.*, 1999, **99**, 3379–3420.
- 9 C. M. Thomas, *Comments Inorg. Chem.*, 2011, **32**, 14–38.
- 10 B. Wu, M. W. Bezpalko, B. M. Foxman and C. M. Thomas, *Chem. Sci.*, 2015, **6**, 2044–2049.
- 11 B. Wu, K. M. Gramigna, M. W. Bezpalko, B. M. Foxman and C. M. Thomas, *Inorg. Chem.*, 2015, **54**, 10909–10917.
- 12 V. N. Setty, W. Zhou, B. M. Foxman and C. M. Thomas, *Inorg. Chem.*, 2011, **50**, 4647–4655.
- 13 B. P. Greenwood, G. T. Rowe, C.-H. Chen, B. M. Foxman and C. M. Thomas, *J. Am. Chem. Soc.*, 2009, **132**, 44–45.
- 14 C. M. Thomas, J. W. Napoline, G. T. Rowe and B. M. Foxman, *Chem. Commun.*, 2010, **46**, 5790–5792.
- 15 B. P. Greenwood, S. I. Forman, G. T. Rowe, C.-H. Chen, B. M. Foxman and C. M. Thomas, *Inorg. Chem.*, 2009, **48**, 6251–6260.
- 16 J. P. Krogman, B. M. Foxman and C. M. Thomas, *Organometallics*, 2015, **34**, 3159–3166.
- 17 B. Oelkers, M. V. Butovskii and R. Kempe, *Chem. – Eur. J.*, 2012, **18**, 13566–13579.
- 18 B. G. Cooper, C. M. Fafard, B. M. Foxman and C. M. Thomas, *Organometallics*, 2010, **29**, 5179–5186.
- 19 S. Kuppaswamy, T. M. Powers, J. P. Krogman, M. W. Bezpalko, B. M. Foxman and C. M. Thomas, *Chem. Sci.*, 2013, **4**, 3557–3565.
- 20 C. Döring, A.-M. Dietel, M. V. Butovskii, V. Bezugly, F. R. Wagner and R. Kempe, *Chem. – Eur. J.*, 2010, **16**, 10679–10683.
- 21 J. W. Napoline, S. J. Kraft, E. M. Matson, P. E. Fanwick, S. C. Bart and C. M. Thomas, *Inorg. Chem.*, 2013, **52**, 12170–12177.
- 22 I. P. Beletskaya, A. Z. Voskoboynikov, E. B. Chuklanova, N. I. Kirillova, A. K. Shestakova, I. N. Parshina, A. I. Gusev and G. K. I. Magomedov, *J. Am. Chem. Soc.*, 1993, **115**, 3156–3166.
- 23 M. V. Butovskii, O. L. Tok, V. Bezugly, F. R. Wagner and R. Kempe, *Angew. Chem., Int. Ed.*, 2011, **50**, 7695–7698.
- 24 M. V. Butovskii, C. Döring, V. Bezugly, F. R. Wagner, Y. Grin and R. Kempe, *Nat. Chem.*, 2010, **2**, 741–744.
- 25 M. V. Butovskii, O. L. Tok, F. R. Wagner and R. Kempe, *Angew. Chem., Int. Ed.*, 2008, **47**, 6469–6472.
- 26 P. L. Arnold, J. McMaster and S. T. Liddle, *Chem. Commun.*, 2009, 818–820, DOI: 10.1039/b819072k.
- 27 M. P. Blake, N. Kaltsoyannis and P. Mountford, *J. Am. Chem. Soc.*, 2011, **133**, 15358–15361.
- 28 A. Spannenberg, M. Oberthür, H. Noss, A. Tillack, P. Arndt and R. Kempe, *Angew. Chem., Int. Ed.*, 1998, **37**, 2079–2082.
- 29 R. Kempe, H. Noss and H. Fuhrmann, *Chem. – Eur. J.*, 2001, **7**, 1630–1636.
- 30 Y. Nakajima and Z. Hou, *Organometallics*, 2009, **28**, 6861–6870.
- 31 F. Völcker, F. M. Mück, K. D. Vogiatzis, K. Fink and P. W. Roesky, *Chem. Commun.*, 2015, **51**, 11761–11764.
- 32 F. Völcker, Dissertation, Karlsruhe Institute of Technology Karlsruhe, 2015.
- 33 F. Völcker, Y. Lan, A. K. Powell and P. W. Roesky, *Dalton Trans.*, 2013, **42**, 11471–11475.
- 34 T. G. Wetzels, S. Dehnen and P. W. Roesky, *Angew. Chem., Int. Ed.*, 1999, **38**, 1086–1088.
- 35 P. W. Roesky, *Heteroat. Chem.*, 2002, **13**, 514–520.
- 36 T. Li, J. Jenter and P. W. Roesky, *Z. Anorg. Allg. Chem.*, 2010, **636**, 2148–2155.
- 37 O. V. Dolomanov, L. J. Bourhis, R. J. Gildea, J. A. K. Howard and H. Puschmann, *J. Appl. Crystallogr.*, 2009, **42**, 339–341.
- 38 D. Fenske, B. Maczek and K. Maczek, *Z. Anorg. Allg. Chem.*, 1997, **623**, 1113–1120.
- 39 M. Enders, B. Görling, A. B. Braun, J. E. Seltenreich, L. F. Reichenbach, K. Rissanen, M. Nieger, B. Luy, U. Schepers and S. Bräse, *Organometallics*, 2014, **33**, 4027–4034.
- 40 S. Ehni and B. Luy, *J. Magn. Reson.*, 2013, **232**, 7–17.
- 41 K. Kobzar, S. Ehni, T. E. Skinner, S. J. Glaser and B. Luy, *J. Magn. Reson.*, 2012, **225**, 142–160.
- 42 N. I. Gershenson, T. E. Skinner, B. Brutscher, N. Khaneja, M. Nimbalkar, B. Luy and S. J. Glaser, *J. Magn. Reson.*, 2008, **192**, 235–243.
- 43 K. Kobzar, T. E. Skinner, N. Khaneja, S. J. Glaser and B. Luy, *J. Magn. Reson.*, 2004, **170**, 236–243.
- 44 T. E. Skinner, T. O. Reiss, B. Luy, N. Khaneja and S. J. Glaser, *J. Magn. Reson.*, 2004, **167**, 68–74.



- 45 T. E. Skinner, T. O. Reiss, B. Luy, N. Khaneja and S. J. Glaser, *J. Magn. Reson.*, 2003, **163**, 8–15.
- 46 M. D. Taylor and C. P. Carter, *J. Inorg. Nucl. Chem.*, 1962, **24**, 387–391.
- 47 M. T. Ashby and Z. Li, *Inorg. Chem.*, 1992, **31**, 1321–1322.
- 48 G. Sheldrick, *Acta Crystallogr., Sect. A: Fundam. Crystallogr.*, 2008, **64**, 112–122.

